Journal of Geophysical Research: Biogeosciences

RESEARCH ARTICLE
10.1029/2018JG004444

Key Points:

- Arctic permafrost tundra ecosystem is an annual net source of CH_4
- Nongrowing season emissions make up 45% of annual CH. loss
- Thaw depth is a significant driver of growing season CH_4 emissions

Supporting Information:
• Supporting Information Sl

Correspondence to:
M.A.Taylor,
meghantaylor@nauedu

Citation:
Taylor,M.A,Celis,G,Ledman,J.D, Bracho,R,& Schuur,E.A.G.(2018). Methane efflux measured by eddy covariance in Alaskan upland tundra undergoing permafrost degradation. *Journal of Geophyskol Research: Biogeosciences*, 123,2695-2710.h ttps://doi.org/10.1029/20 18JG004444

Received 11 FEB 2018
Accepted 11JUL 2018
Accepted article online 17JUL 2018
Published online 7 SEP 2018

Methane Efflux Measured by Eddy Covariance in Alaskan Upland Tundra Undergoing Permafrost Degradation

M.A. Taylor[1], G.Celis[1], J.D. Ledman[12], R. Bracho[3] and E. A. G.Schuur[1]

'Center for Ecosystem Society and Science (ECOSS), Northern Arizona University, Flagstaff, AZ, USA, [2]Bonanza Creek Long Term Ecological Research Site, University of Alaska, Fairbanks, AK, USA, [3]School of Forest Resources and Conservation, University of Florida, Gainesville, Fl,USA

Abstract Greenhouse gas emissions from thawing permafrost in arctic ecosystems may amplify global warming, yet estimates of the rate of carbon release, and the proportion of carbon released as methane (CH_4) or carbon dioxide (CO:i), have a high degree of uncertainty.There are many areas where no measurements exist, and few year-round or long-term records.Existing year-round eddy covariance measurements of arctic CH_4 fluxes suggest that nongrowing season emissions make up a significant proportion of tundra systems emissions on an annual basis. Here we present continuous CH_4 flux measurements made at Eight Mile Lake,an upland tundra ecosystem undergoing permafrost degradation in Interior Alaska. We found net CH_4 emissions throughout the year (1.2 + 0.011 g C-CH_4 m^2/yr) that made up 61% of total radiative forcing from annual C emissions ($C0_2$ and CH.i; 32.3 g C m^2/yr) when taking into account the greenhouse warming potential of CH_4 relative to COi. Nongrowing season emissions accounted for 50% of the annual CH_4 budget, characterized by large pulse emissions. These were related to abrupt increases in air and shallow soil temperatures rather than consistent emissions during the zero curtain-a period of the fall/early winter season when subsurface soil temperatures remain near the 0 °C freezing point. Weekly growing season CH_4 emissions in 2016 and 2017 were significantly related with thaw depth, and the magnitude of CH_4 emissions between these seasons was proportional to the rate of active layer thaw throughout the season.

1. Introduction

Arctic warming exposes a portion of the estimated 1,330-1,580 Pg of permafrost carbon pool to potential microbial decomposition as previously frozen ground thaws (Hugelius et al., 2014;Schuur et al., 2015). Organic carbon (C) stored within permafrost zone soils can be released as greenhouse gases (GHGs), and it is critical to be able to estimate how much will be released via aerobic decomposition as carbon dioxide (CO:i) or anaerobic decomposition as methane (CH_4) and $C0_2$ (Schuur et al.,2008). This is because sustained CH_4 emissions have 45 times the radiative forcing of $C0_2$ over a 100-year time scale and may therefore have a significant effect on the GHG warming potential from high-latitude terrestrial ecosystems (Myhre et al.,2013; Neubauer & Megonigal,2015). The fraction of C released as CH_4 will be dictated in large part by the changing hydrology of Arctic systems, where newly waterlogged areas may produce CH_4 anaerobically even in regions not usually associated with net methane emissions, for example, relatively well drained upland tundra (Natali et al.,2015;Nauta et al.,2015;Olefeldt et al., 2016).

Degradation of permafrost by rising air temperatures creates ground subsidence (Grosse et al.,2011) that can lead to land surface collapse in ice-rich permafrost in a process called thermokarst. Thermokarst landscape is estimated to cover 20% of the northern permafrost terrain (Olefeldt et al., 2016). Thaw and the resulting subsidence create changes in microtopography where water drains to regions of low relief, while higher areas drain and become drier. Deeper permafrost thaw may occur as a positive feedback in low-lying areas via increased thermal erosion from pooled water in summer and increased snow accumulation that insulates soils in winter (Blanc-Betes et al.,2016;Johansson et al.,2013). Increased ground subsidence may also shift some upland areas to stronger CH_4 sources (Natali et al.,2015;Nauta et al., 2015). Changes in soil moisture in response to permafrost thaw is a major source of uncertainty in projecting long-term trends of CH_4 emissions and the amplitude of GHG responses (Lawrence et al.,2015;Treat et al.,2015).

Arctic tundra systems account for an estimated 19 Tg/yr of global CH_4 emissions at present, but there are large uncertainties (8-29 Tg/yr) owing to scarce spatial coverage and the paucity of year-round or

long-term records (McGuire et al.,2012). The few studies with data coverage outside of the growing season indicate that emissions during the nongrowing season may be significant, comprising up to half of the annual emissions in some sites. Several studies have shown large CH_4 emissions relative to annual emissions during a period of the shoulder season with incomplete soil freeze up known as the zero curtain (Outcalt et al., 1990; Zona et al.,2016), during spring thaw (Raz-Yaseef et al.,2017), or autumn freeze (Mastepanov et al., 2008;Pirk et al.,2015;Whalen & Reeburgh, 1988).The zero curtain effect is the observed delay in refreezing of the active layer in permafrost affected soils. The zero curtain occurs as a result of the latent heat of unfrozen soil water that maintains soil temperatures near 0 °C(Outcalt et al.,1990;Romanovsky & Osterkamp,2000). Dry tundra ecosystems have been reported to be potentially significant CH_4 sinks (D1mperio et al., 2016;J0rgensen et al., 2014) or low-level sources (Euskirchen et al., 2016;Whalen et al., 1991).However,taking into account this zero curtain period, recent work has shown that late-season CH_4 emissions in dry tundra during the can be substantial (Zona et al., 2016). As a result, much of the uncertainty in annual arctic CH_4 assessments lies in emission estimates from the nongrowing season. Large uncertainties in CH_4 emissions estimates complicate efforts at process-based upscaling of CH_4 flux measurements and modeling the potential response of CH_4 fluxes to the effects of climate change-particularly as future Arctic warming is likely to be skewed during the spring and winter months when measurements are lacking (Bekryaev et al.,2010).

Eight Mile Lake near Healy,AK,is an upland tussock tundra site that has been undergoing thermokarst for several decades (Osterkamp et al., 2009). Permafrost degradation has resulted in heterogeneous ground subsidence that has affected surface hydrology and soil temperatures, as well as shifting plant species composition from tussock forming sedges to shrub species in areas of increased thaw (Belshe et al.,2012; Schuur et al.,2007). Carbon dioxide fluxes from the site have been characterized using chamber-based and eddy covariance data collection since 2004 (Belshe et al., 2012;Celis et al., 2017;Lee et al., 2011; Trucco et al.,2012;Vogel et al., 2009). Thawing of permafrost at Eight Mile Lake (EML) has amplified the COi-C cycle during the growing season, stimulating photosynthesis and ecosystem respiration and shifting EML from a historically net sink to $C0_2$ neutrality like other sites within the tundra biome (Belshe et al., 2012;Hicks Pries et al., 2012;Belshe et al., 2013b), and a net source of $C0_2$ on an annual basis due to nonsummer season emissions (Celis et al.,2017).

Here we present eddy covariance CH_4 measurements made from April 2016 to October 2017. Our objective with this study is to understand the magnitude, seasonality,and relative importance of $C0_2$ and CH_4 fluxes with the addition of year-round CH_4 eddy covariance measurements. We anticipate that CH_4 uptake might dominate the growing season,and any positive net fluxes during the growing season would likely be greatest in July, when environmental drivers that typically control CH_4 fluxes and promote CH_4 production and transport like soil moisture and temperatures, cumulative precipitation, and peak biomass were most favorable. During the fall/early winter,we expected CH_4 fluxes to constitute a net source. While EML does not experience widespread surface inundation, surface subsidence and thermokarst development from permafrost thaw are important predictors of summer season $C0_2$ fluxes at EML (Lee et al., 2011;Mauritz et al., 2017), and experimental permafrost thaw near EML has shown that increased ground subsidence significantly increased CH_4 emissions (Natali et al.,2015). Changes in soil moisture with permafrost thaw have the potential to significantly change the C dynamics and the form of C released via respiration.

2. Methods

2.1. Site Description

This study was conducted within the Eight Mile Lake watershed (63°52'42"N, 149°13'12"W), in the northern foothills of the Alaska Range near Denali National Park and Preserve.The study site is located at 700-m elevation on a gentle hillslope (-5%;Belshe et al.,2013b). Surface soils are relatively well drained and consist of *05* m of organic soils overlying mineral soil made up of glacial till and loess deposits (Osterkamp et al., 2009; Schuur et al., 2009;Vogel et al., 2009). The upland tundra vegetation forms an open canopy and is dominated by low, dwarf shrubs (e.g., *Betula nana* and *Vaccinium uliginosum),* tussock forming sedges *(Eriophorum vaginatum),* and mosses and lichen (CAVM Team, 2003;Schuur et al.,2007). This site is underlain by permafrost and colocated with a 30-m deep borehole where permafrost temperatures have been recorded since 1985 (Osterkamp & Romanovsky, 1999). Permafrost temperatures have increased by 0.5 °C, and thermokarst terrain (ground subsidence) has expanded during this interval (Belshe et al.,2013a;Osterkamp et al., 2009).

2.2. Environmental Monitoring

Meteorological data included photosynthetically active radiation (PAR;PQSl Kipp & Zonen),incident and net radiation (CNR4 Kipp & Zonen), relative humidity and air temperature (Vaisala HMP45C,Campbell Scientific), wind speed and direction (RM Young 3001, Campbell Scientific), snow depth (SR50A,Campbell Scientific), and soil moisture at 15-cm depth (Stevens Hydra probe II,Stevens Water Monitoring Systems). All data were recorded with a Sutron 9210-Xlite data logger (Sutron Corporation). A replicate set of micrometeorological data sensors including PAR,air temperature and relative humidity,and soil temperature were measured at a second tower located 100 m to the NW of the eddy covariance (EQ tower and were used to fill gaps in meteorological data. Soil temperatures were measured at multiple depths (5, 10, 15,20,30, 40, and 60 cm) using type constantan-copper thermocouples at nine sites within the tower footprint and at two sites with thermistors at the EC tower. Soil moisture was integrated over the top 15 cm of soil, measured with 11 water content reflectometers within the tower footprint and 2 at the EC tower (CS615 and CS616, Campbell Scientific). Temperature and moisture were measured every 5 min and averaged at half-hourly intervals, recorded by a data logger (CRIOOO,Campbell Scientific). Rainfall was measured using a HOBO Onset station during the growing season (Bourne, MA, USA). Thaw depth was measured biweekly during the growing season at nine locations within the tower footprint using a metal depth probe. Water table depth (WTD) was measured at the same frequency at nine wells as described in Vogel et al. (2009).

2.3. Flux Measurements

Landscape level carbon (C-CH_4 & C-CO:i) fluxes were measured from April 2016 to October 2017 using the eddy covariance (EQ method. The EC system consisted of a sonic anemometer (CSAT3, Campbell Scientific), an open-path CH_4 analyzer (Li-7700, U-COR Biosciences), and an open-path $C0_2$ analyzer (Li-7500A, U-COR Biosciences) mounted on a *35-m* tower. The EC tower fetch is approximately 900 m east, west, and north and about 400 m south.The estimated area contributing to 80% of the measured fluxes-footprint-was -160 m in the summer season (May to September) and about 230 m in the nonsummer season (October to April; Figure SI in the supporting information;Kljun et al., 2004; Kormann & Meixner, 2001). Vegetation within the tower footprint is relatively uniform and dominated by low shrubs *(Betula nana* and *Vaccinium uglinosum)* and tussock tundra *(Eriophorum vaginatum).* Eight Mile Lake is to the north of the tower and does not fall within the tower footprint. There is thermokarst at the site that was described in Belshe et al. (2013b), with microtopography variation of -0.2 to 0.2 m in reference to tower, and a gentle hillslope (-5%). Vegetation in thermokarsted area is similar to nonthermokarst. We would therefore describe the site as homogenous in topography and vegetation height and composition. Methane, $C0_{21}$ water vapor, orthogonal wind components (u, v, and w), and air temperature were recorded at 10 Hz using a U-7550 Analyzer Interface Unit (LiCOR Biosciences). The CH_4 analyzer and $C0_2$ analyzers were calibrated twice a year using a zero CH_4 and $C0_2$ air source,an atmospheric CH_4 standard (Ameriflux,1.9022 ± 0.0 ppm) for the CH_4 analyzer, and an atmospheric $C0_2$ standard (Ameriflux,401.71 ± 0.003 ppm) for the $C0_2$ analyzer. A dew point generator (Li-610, LI-COR Biosciences) was used to calibrate for water vapor.

We used EddyPro v6.2.0 software (LI-COR,2017) to process and apply corrections to the high-frequency data, which were then aggregated to half-hourly fluxes. High-frequency data were corrected for (1) wind axis double ration method (Aubinet et al., 2000; Foken & Wichura, 1996); (2) time lag with covariance maximization; (3) statistical test following Vickers and Mahrt (1997), which includes accepted spikes at 1% and replaced with linear interpolation with plausible ranges of wind was 5 standard deviations (SD), H_20 and $C0_2$ were 3.5 SD, and CH_4 was 8.0 SD;(4) frequency loss;(5) sensor separation; and (6) air density (Burba et al., 2008; Webb et al., 1980). Postprocessing screening eliminated data when (1) less than 90% of the high-frequency data were collected in the 30-min interval, (2) frictional speed (U*) was <0.1 m/s (Goulden et al., 1996), (3) raining conditions when sensor signal dropped below 70% LI-7500A and 10% LI-7700, and (4) periods of sensor calibrations. Data *QNQC* flagging was based on steady state and developed turbulence tests (Mauder & Foken, 2006), resulting in three levels of data quality (0 = high, 1 = intermediate, and 2 = poor) and all data with level 2 flags were discarded.

2.4. Gap Filling

Data gaps were filled using the marginal distribution sampling (MDS) algorithm (Reichstein et al., 2005) in REddyProc (Wutzler et al., 2018) that excluded data >2 standard deviations from the overall mean of the

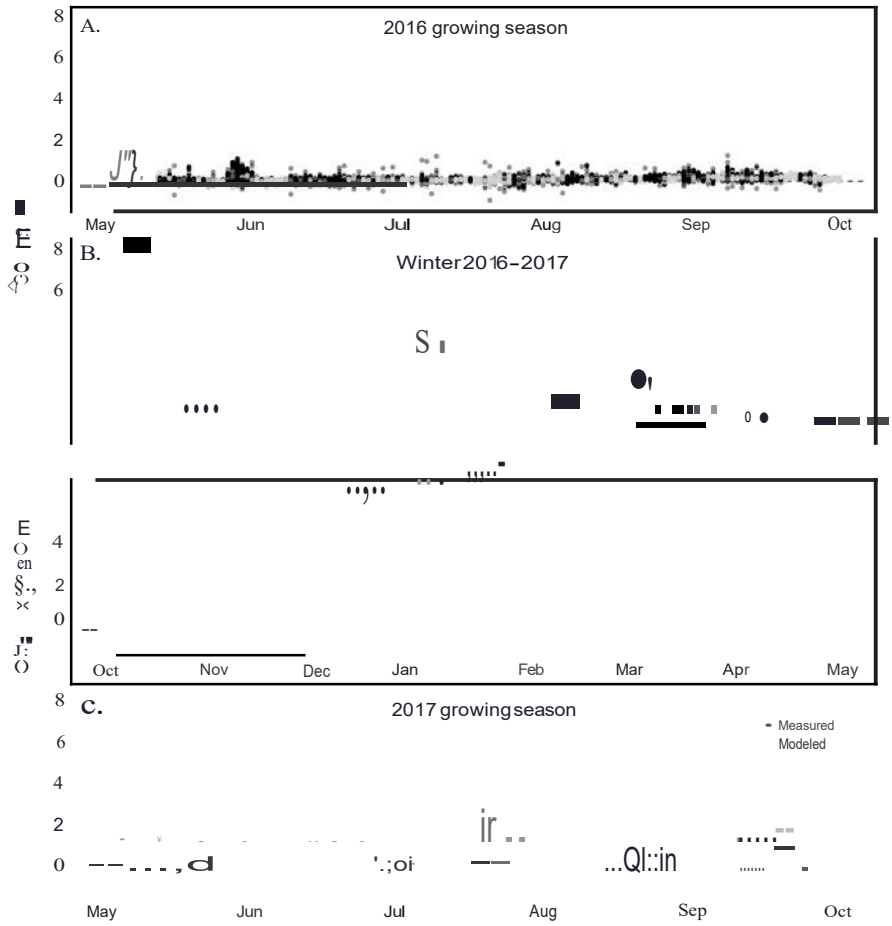

Figure 1. Measured (dark filled circles) and gap filled (light gray filled circles) half-hourly eddy covariance CH4 fluxes from (a) the 2016 growing season (May-September), (b) the winter season (October 2016 to May 2017), and (c) the 2017 growing season (May-September).

data set to exclude methane outbursts ($N = 240$) that could not be explained by any environmental data. The MDS algorithm takes into account the covariation of fluxes with environmental variables and the temporal autocorrelation of the fluxes based on (1) look-up table and (2) the mean diurnal course (Wutzler et al., 2018). The environmental variables used were air and 5-20-cm depth soil temperatures, soil volumetric water content, wind speed, and air pressure, and details of the specific temporal window sizes and variable selection can be found in supporting information (Table SI). The average postprocessing data coverage after filtering was applied for the measurement period was 35.5% across all; the seasonal distribution of the data coverage is shown in Figure S2. Measured versus modeled data are shown in Figure 1. The gap filling of CO_2 fluxes is as described in Celis et al., 2017.

2.5. Error Estimation

Random measurement uncertainties were estimated using the "daily differencing approach" (Hollinger & Richardson, 2005), which uses measured fluxes under similar environmental condition at the same time of day in a 2-day window (Figure 53). Environmental variables used and threshold for determining similar environmental conditions were air temperature (3 °q, photosynthetic active radiation (PAR; 75 μmol $\cdot m^2 \cdot s$) and wind speed (1 mis; Table SI). Gap-fill uncertainties by the MDS algorithm were estimated determining the difference between measured and gap-fill value of the artificial gap created by MDS (Wutzler et al., 2018; Table 1). We summed and propagated the random and gap-fill uncertainties over time.

2.6. Data Analysis

Two sets of analyses were conducted: one with year-round data (1 May 2016 to 1 May 2017) and another with both growing seasons. This was because there were more variables that could be incorporated into the growing season models and only three variables that were measured year-round. For these analyses, growing seasons began when daily averaged soil profile temperatures from 5 to 60 cm were above 0.1 °C (spring thaw) and ended when daily averaged soil temperatures dropped below -0.1 °C (fall freeze in). In 2016, this interval was 21 April to 8 October, and in 2017 it was 5 May to 1 October.

Table 1
Methane Flux Uncertainty Estimate (Standard Deviation of the Error) for Measurements and Gap-Filled Data

	Random error C-CH$_4$ mg/m^2 per period				Gap-filled error C-CH$_4$ mg/m^2 per period			
Period	*N*	Mean	SD	SE	*N*	Mean	SD	SE
Summer	467	0.11	5.90	0.27	6377	254.73	289.36	3.62
Winter	327	0.26	4.41	0.24	4470	248.96	298.38	4.46
Overall	794	0.56	19.73	0.70	10847	889.35	1049.08	10.07

Note. Random error inferred using daily differencing approach (Richardson et al., 2006) and gap-filled method using difference of modeled versus measured data.

The relationship between median weekly CH_4 fluxes and environmental variables measured year round (shallow and deep soil temperatures and soil moisture) were evaluated using linear regression. We used a backward stepwise model selection to identify significant environmental drivers. A five-point improvement of the Akaike Information Criterion (AIC) was used to justify a more complex model. There appears to be a lagged effect of soil temperatures on CH_4 emissions, where emissions respond to the driving variable-soil temperatures-differently in different seasons. In early spring, low soil temperatures are associated with low emissions, while late as soil temperatures decline in the summer and early fall season, emissions still increase. To characterize the apparent lag between weekly median CH_4 fluxes and shallow and deep soil temperatures, hysteretic ellipses were fit using direct specific least squares method (hysteresis; Maynes et al., 2017). All analyses were conducted in R (RCore Team, 2017). Pulses, or CH_4 pulse emissions, constituted *43%* of the measured data and were not linearly related with environmental drivers (Table S2) on an annual basis. As a result, these values were excluded from the linear regression analyses of the annual data. Pulses were defined and removed on the basis of fluxes measured greater than 2 standard deviations from an overall mean: if these outlier fluxes measured during a day exceeded numbered greater than or equal to 4 (or 2 hr of outlier fluxes), it was considered an outburst emission and was excluded from linear analyses.

Linear mixed models (nlme; Pinheiro et al., 2017) were used to analyze the relationship between weekly median growing season CH_4 fluxes and environmental drivers (thaw depth, WTD, shallow [5-15 cm] and deep soil [20-60 cm] temperatures, cumulative precipitation, and soil moisture). The model included year as a random effect in order to account for interannual variability. We used a backward stepwise model selection to identify significant environmental drivers. A backward stepwise model selection was used as described in the linear regression analyses. A five-point improvement of the AIC was used to justify a more complex model.

Emissions calculations.

Methane emissions are reported in g C-CH_4. In order to report total C emissions at EML, we calculated the CO_2 equivalent of CH_4 by multiplying CH_4 by its 100-year sustained emissions global warming potential of 45 after accounting for the mass difference between CH_4 and CO_2 gases (Neubauer & Megonigal, 2015).

3. Results

3.1. Environmental Conditions

Average annual air temperature from May 2016 to April 2017 was -1.0 °C, the same as the long-term mean (1977-2016; -0.93 ± 0.24 °C) for the site (Figure 2h). Maximum active layer thickness in 2016 was 68.6 ± 1.3 cm in 2016 and 66.2 ± 2.0 cm in 2017 (Figure 2f). Maximum snow depth was 0.54 m in winter of 2016-2017, and the site was snow free by 30 April 2017. The 2016 growing season was wetter than 2017 with higher cumulative rainfall by 254.4 mm and higher soil moisture by 6% (Table 2 and Figure 2b). Peak rainfall occurred in July in both years. In 2016, depth to water table throughout the growing season was consistently 6-12 cm below the soil surface (Figure 2a). In 2017, WTD fluctuated between 12 and 17 cm, except in May after snowmelt when average depth to water table was 4 cm (Figure 2a). Mean shallow (5-15-cm) and deep (20-60-cm) soil temperatures were warmer in 2016 by 0.73 and 0.54 °C respectively, and mean air temperatures were warmer in 2017 by 0.80 °C (Table 2 and Figures 2g and 2h).

Maximum snow depth measurements starting in 2012 varied between 0.68 cm (winter 2012-2013) to 033 cm (winter 2014-2015; Table 3). The date of consistent snow accumulation >20 cm ranged from the

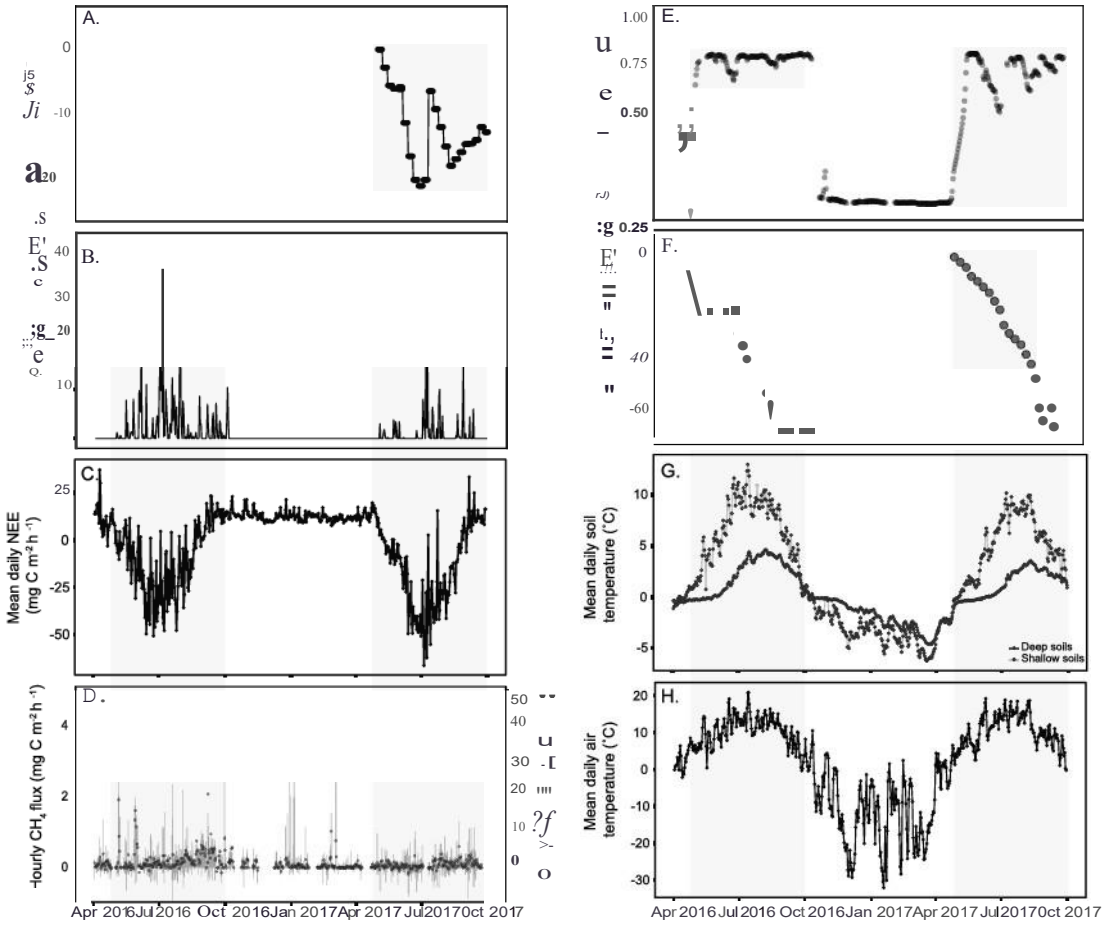

Figure 2. Eddy covariance and environmental variables measured in 2016-2017 at Eight Mile Lake: (a) weekly depth to water table, (b) cumulative daily summer precipitation, (c) mean daily net ecosystem exchange, (cf) hourly (gray line) and daily (red circles) CH_4 flux, (e) volumetric water content, (f) weekly thaw depth, (g) mean daily shallow (5-15-cm) and deep (20-60-Cm) soil temperatures, and (h) mean daily air temperature.

first week in October 2014 to 3 months later in the year, in January 2017 (Table 3). Zero curtain length was calculated as the number of days the daily average soil temperatures remained between 0.75 and -0.75 °C. The zero curtain was calculated from shallow (5-15-cm) and deep (20-60-cm) soil temperatures during the fall shoulder season (6 October 2016 to 12 January 2017). There was large interannual variability in the zero curtain length (Table 3) of shallow soil temperatures, while zero curtain length in deep soil temperatures decreased from ~150 days in the shoulder seasons of 2012 and 2013 to 72 days in 2016.

Table 2
Environmental Variables Measured at the Site Annually and During the Growing Seasons of 2016 and 2017

Variable	May-September 2016	May-September 2017	Annual 2016/2017
Mean air temperature (°C)	9.94 (0.06)	10.74 (0.06)	-1.02 (0.10)
Mean shallow (5-15 cm) Soil temperature (°C)	6.10 (0.04)	5.37 (0.03)	1.04 (0.04)
Mean shallow (20-60-cm) soil temperature (°C)	1.98 (0.02)	1.44 (0.02)	-0.11 (0.02)
Cumulative precipitation (mm)	411.2	156.8	414.2
Mean volumetric water content (%)	0.76 (0.001)	0.70 (0.002)	0.39 (0.003)
Mean water table depth (cm)	8.72 (0.86)	12.14 (1.15)	
Active layer thickness (cm)	68.56 (1.28)	66.16 (2.00)	

Note. Values in parentheses are standard error.

Table 3
Winter Season Snow Depths, Date of Snow Acrumulation >02 m, and Length of the Zero Curtain Based On Daily Mean Shallow (5-10 cm)

Winter	Maximum snow depth (m)	Date of snow accumulation	Zero curtain length (days)	
			Shallow soil temperatures	Deep soil temperatures
2012-2013	0.68	16 October 2012	51	148
2013-2014	0.36	30 November 2013	119	172
2014-2015	0.33	8 October 2014	79	114
2015-2016	0.41	30 October 2015	65	120
2016-2017	0.54	4 January 2017	51	72

3.2. Annual CH_4 Emissions

The Eight Mile Lake EC site was a net source of CH_4 emissions on an annual basis (1 May 2016 to May 2017) with cumulative emissions of 12 + 0.011 g C-CH_4 m^2/yr. Emissions occurred year round, with 55% of emissions during the growing season and 45% during the shoulder and winter season. Net methane uptake also occurred during sampling intervals and comprised 9.2o/o of total net C exchange (total mg C-CH_4 m^2/yr; Table 4). The zero curtain averaged across all soil depths lasted for 81 days (29 September to 19 December 2016, and emissions during that period were 22% of the annual CH_4 budget and 45% of winter emissions. Methane pulses occurred during spring thaw and also during December 2016 to January 2017. The midwinter pulses coincided with air warming from -29 °C to -2.7 °C in mid-December and surface soil warming from -45 °C to -2.2 °C on 1 January 2017 (Figures 2d, 2g, 2h, 3d, and 4). Starting 24 December 2016, emissions increased from 2.2 mg C-CH_4 m^2/day and culminating in 2 days where emissions were between 43.9 and 47.4 mg C-CH_4 m^2/day (Figure 4). At EML, winter pulses were rapid, and transient, while spring thaw pulses lasted up to a week of consistently high values (Figure 4). Pulses made up 21% of the annual gap filled budget.

A subset of environmental variables measured year round was used to evaluate the response of annual median weekly CH_4 fluxes from 1 May 2016 to 1 May 2017 to changes in shallow and deep soil temperatures and soil moisture. All of these variables were significant drivers of annual emissions (conditional adjusted $R2$ = 053; Figure 5 and Table 5). Methane fluxes increased with increased deep soil temperatures and soil moisture, while fluxes decreased with increased shallow soil temperatures (Table 5 and Figure 5). The annual hysteretic cycle of CH_4 fluxes in response to shallow soil temperatures resulted in an ellipse with an area of 1.56, while the area of the ellipse fit to the annual hysteretic cycle of CH_4 fluxes in response to deep soil temperatures was 0.65 (Figure 5). The widest hysteresis between shallow soil temperatures and resultant CH_4 fluxes occurred between spring (weeks 20-24; 23 May to 19 June) and early fall (weeks 35-38, 29 August to 25 September) in 2016 when shallow soil temperatures were 5.3 °C ± 13. At the same temperatures, CH_4 fluxes were low during the spring (0.0295 ± O.QI 3) and highest during the early fall (0.170 ± 0.012). The exception is during week 22, when median fluxes were similar to fall fluxes, probably due to spring thaw CH_4 release.

Table 4
Proportion of Season and Annual CH_4 Uptake and Release

Season	Number of measured fluxes (30 min)	Total CH4 mg	Total exchange by mass (%)
Growing 2016 (1 May 2016 to 30 September 2016)			
Uptake	580	-48.67	10.6
Release	2,434	410.49	89.4
Growing 2017 (1 May 2017 to 30 September 2017)			
Uptake	1,174	-69.5	27.2
Release	2,337	186.29	72.8
Nonrowing 2016/2017 (1 October 2017 to 30 April 2017)			
Uptake	456	-18.40	6.9
Release	1,835	249.8	93.1
Annual Calendar 2016/2017 (1 May 2016 to 30 April 2017)			
Uptake	1,036	-67.06	9.2
Release	4,269	660.29	90.8

3.3. Drivers of Growing Season 2016 and 2017 CH_4 Emissions

Spring thaw began on 21 April 2016. Higher emissions between 5.7 and 18.5 mg C-CH_4 m^2/day were observed between 5 May 2016 and 1 June 2016 (Figures 3b and 3c). While these emissions were ephemeral, they constituted 99.7 mg C-CH_4 m^2/day or 125% of the 2016 growing season budget within 21% of the growing season. There was a strong diurnal pattern to these larger spring thaw emissions that began 15 days after the onset of soil column thaw. In 2017, there was no evidence for large thaw emissions during May and June (Figure 3a).

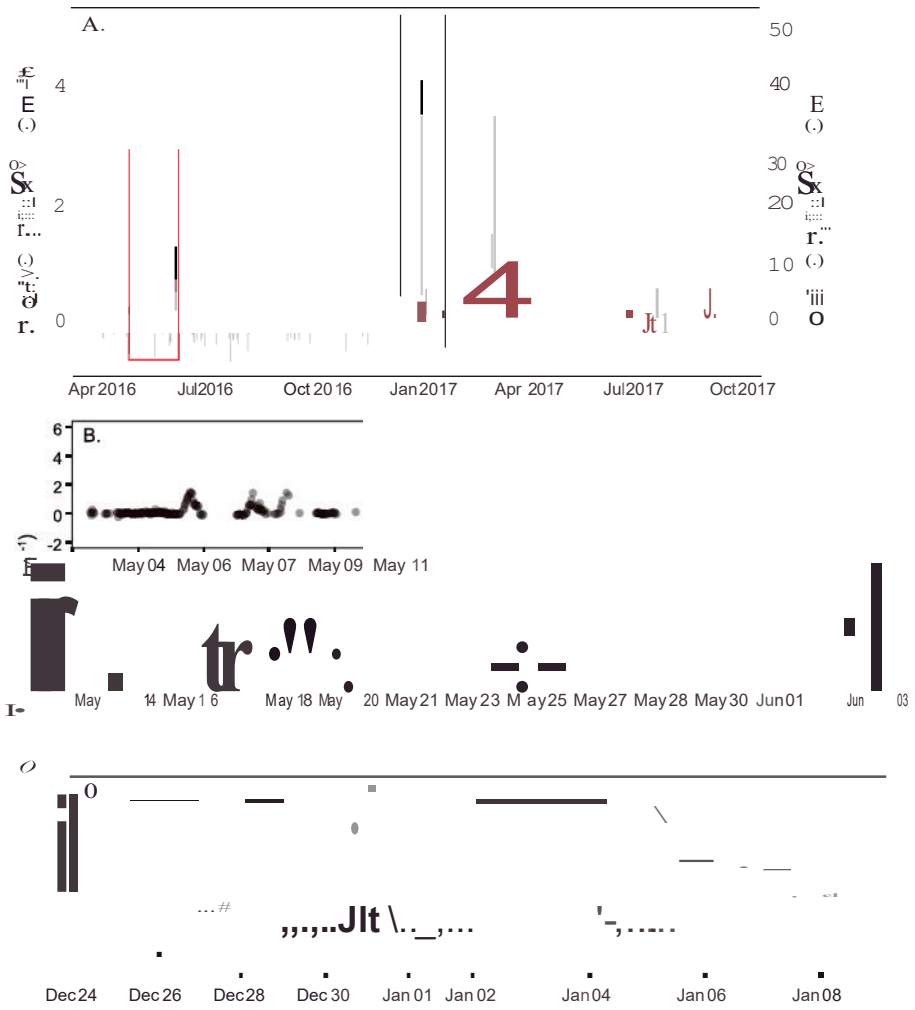

Figure 3. Year-round eddy covariance measured fluxes (a) hourly (gray line) and daily (red circles) CH4 fluxes and (b and c) half hourly EC CH_4 fluxes during spring thaw 2016 events (from red inset box in panel (a) and during (d) winter 2016/2017 outburst events (from black inset box in panel (a)).

Measured fluxes showed a net release of CH_4 during both growing seasons, but uptake also occurred, accounting for 10.6% and 27.2% of total CH_4 exchange (total mg C-CH_4 m^2/yr) during 2016 and 2017, respectively (Table 4). Cumulative growing season (1 May to 30 September) emissions were ~2 times higher in 2016 (653.3 ± 3.9 mg C-CH_4) than 2017 (280.2 ± 3.9 mg C-CH_4). Peak emissions occurred during the week of 29 August in 2016 and during the week of 21 August in 2017 (Figure 2d).

We evaluated the response of weekly median growing season CH_4 fluxes to changes in thaw depth, WTD, shallow and deep soil temperatures, cumulative precipitation, and soil moisture using linear mixed effects modeling. The best fit reduced model included thaw depth and WTDs as explanatory variables for weekly median CH_4 fluxes. Thaw depth has a strong, significant linear relationship in both 2016 and 2017 (conditional adjusted R^2 = 0.61; Figure 6 and Table 6), while WTD is weakly related (not significant) with median CH_4 fluxes.

4. Discussion

4.1. Annual CH_4 Emissions

In this study, we found that CH_4 emission was greater than uptake, and therefore, EML was a net landscape source during both the growing and nongrowing seasons. Accounting for the global warming potential of CH_4 compared to CO_2, annual CH_4 emissions at EML were equivalent to annual CO_2 losses. The first year of cumulative CH_4 emissions (1.2 ± 0.011 g C-CH_4 m^{-2}) measured at EML falls within ranges measured at other

sites. At an upland tundra site in northern Alaska emissions during the growing season were 1.9-2.7 g $C\text{-}CH_4\ m^{-2}$ (Zona et al., 2016) and across wet sedge to dry heath arctic tundra emissions ranged from 0.95

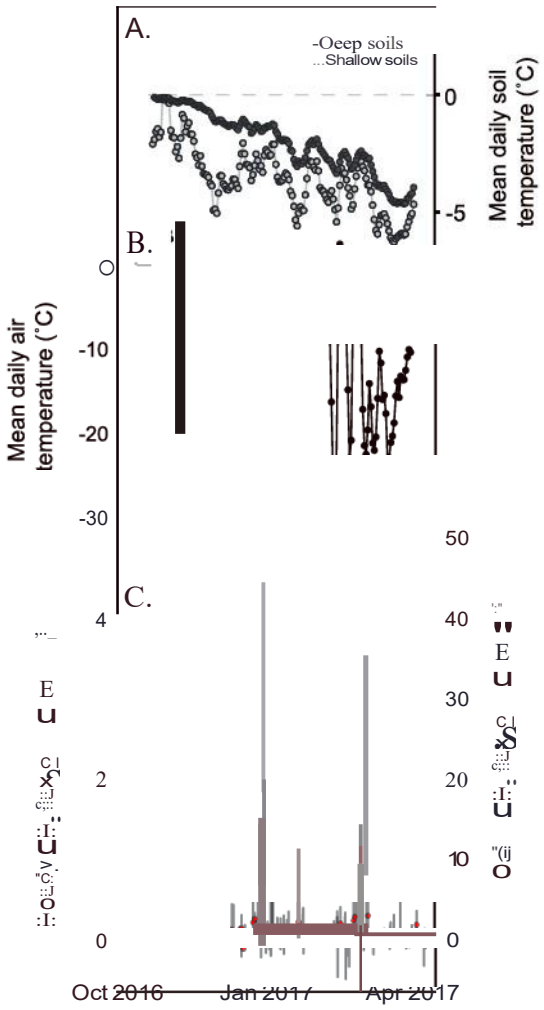

Figure 4.Eddy covariance and environmental variables measured during December-January 2016-2017 at Eight Mile Lake: (a) mean daily shallow (5-15-cm) and deep (20-6Ckm) soil temperatures,(b) mean daily air temperature, (c) hourly (gray line) and daily (red circles) CH_4 flux.

to 1.7 g C-CH_4 m-^{2} (Euskirchen et al., 2016). Wet meadow tundra site emissions during the growing season were 3.15-4.4 g C-CH_4 m-^{2}, while autumn fluxes were 1.1 g C-CH_4 m-^{2} (Sturtevant et al., 2012;Wille et al., 2008). In high-latitude arctic tundra, growing season fluxes were highly variable (1.42-4.09 g C-CH_4 m-^{2} over 5 years, as were nongrowing season fluxes (0.02-3.76 g C-CH_4 m-^{2} Mastepanov et al., 2013).

Analyses of drivers of CH_4 emissions on an annual basis (1 May 2016 to 1 May 2017) showed that soil temperatures and moisture were all significant factors driving CH_4 emissions. Methane emissions integrate several processes that control methanogenesis, methanotrophy, and transport to the atmosphere. Soil temperature is known to be an important control on microbial metabolism and therefore the balance of methane production and consumption, while soil moisture controls the availability of anaerobic microsites for CH_4 production (Christensen et al., 2003). Emissions may also be mediated by the presence of graminoid vegetation, which promotes CH_4 transport to the atmosphere (King et al., 1998). Methane gas produced at depth can bypass oxidation in soils by rapid transport to the atmosphere via vascular plant stem tissues, and this process has been shown to be an important factor for CH_4 emissions in drier sites (Davidson et al.,2016;McEwing et al., 2015).

However, at EML, drivers of CH_4 fluxes also varied seasonally. There is also strong evidence that emissions were strongly influenced by preceding events-that the dynamics of snow depth, soil temperatures, and winter warming events affected the timing and magnitude of CH_4 efflux throughout the year. This was especially important for pulse events, which made up a significant proportion (~22o*b*) of the annual CH_4 budget.

4.2. Snow Depth and Zero Curtain Emissions

Late winter snow accumulation at EML likely affected the rate of surface soil temperature freeze in. Over the last 5 years of measured data, earlier snow accumulation led to longer zero curtain periods and warmer surface soils (Table 3). Snowfall and accumulation usually occurred between October and November and remained at relatively constant depth until spring thaw. During the 2016-2017 winter, thin snow cover repeatedly melted until January when snow accumulation increased rapidly (Figure 54). As a result, both deep and shallow soil temperatures refroze relatively rapidly, reaching temperatures below -1 °C by mid-October. We hypothesize that low zero curtain CH_4 emissions during the winter of 2016-2017 were characterized by a relatively late snow accumulation that resulted in very cold shoulder season surface soil temperatures even while maximum snow depth (O.S4 m) was within range of recorded depths at this site. Recent work has shown that the zero curtain period can be a significant source of CH_4 emissions (2.4-2.1 g C-CH_4 m-^{2} or 32o*b* of the annual budget) in upland tundra at Ivotuk, on the North slope of Alaska (Zona et al., 2016), where soil temperatures remain near 0 °C for as many days as the growing season length. At Ivotuk, this is credited in part to relatively deep winter snow (0.4 m depth) that insulates soil temperatures during the shoulder season. We suggest that zero curtain emissions might be in similar sites to EML like Ivotuk may also be affected by rate of surface soil freeze in as mediated by the timingtfgap of snow cover and accumulation.

Increasing interannual and regional heterogeneity with respect to snow depth and rates of accumulation are likely (Zhang, 2005), and while global climate models predict increased high-latitude precipitation with increased Arctic warming (Zhang et al.,2013;Bintanja & Selten,2014), snow cover duration in Alaska is also projected to decline through 2050 (Callaghan et al.,2011). The potential sensitivity of nongrowing season emissions to drivers like timing of snow accumulation underscores the need for more CH_4 measurements in tundra systems to understand these interactions over longer time scales.

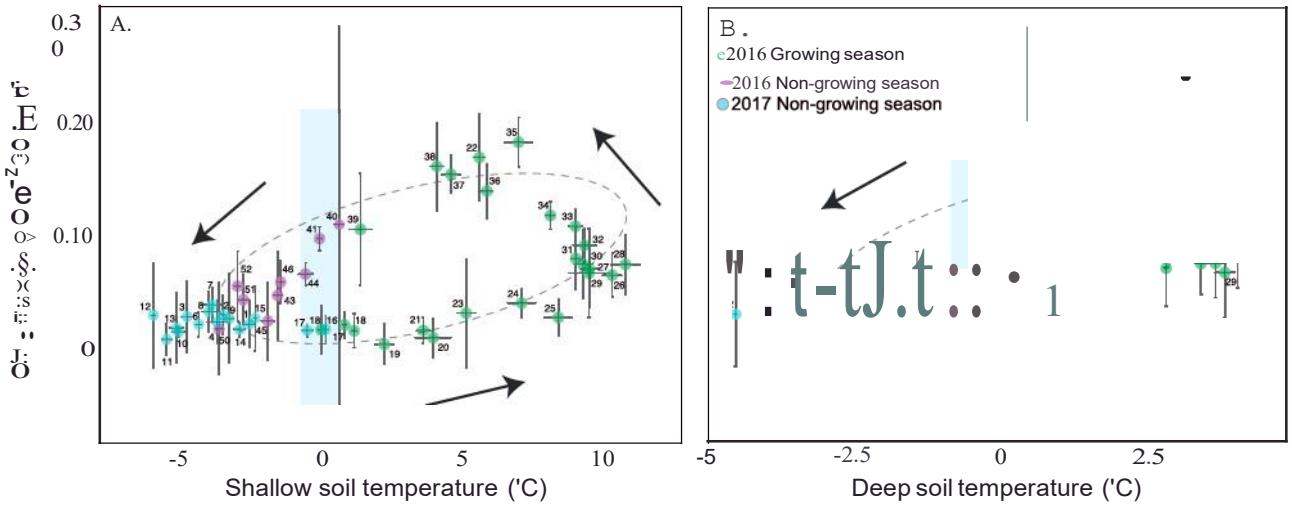

Figure 5. Weekly mean (a) shallow (5-15-cm) and (b) deep (20-60-cm) soil temperatures plotted against median weekly CH4 fluxes. Light blue reflects zero curtain soil temperatures. Filled circle colors refer to different seasons and years measured, and points are labeled by the week of the year they were measured. Arrows represent seasonal progression of temperatures from May 2016 to May 2017. Hysteresis ellipses were fit using direct specific least squares method.

4.3. Effects of Preceding Events on CH_4 Emissions

Seasonal patterns of CH_4 emissions vary among sites in the Arctic. Significant emissions during spring and autumn are a common feature in high-frequency time series and often coincide with snowmelt or soil freeze events (Sturtevant et al., 2012; Raz-Yaseef et al., 2017; Zona et al., 2016; Pirk et al., 2017). Spring thaw emissions may result from the release of previously produced shoulder season CH_4, trapped in frozen soils. Release has been observed by thawing surface soils shortly after snowmelt or prior to snowmelt as a result of rain on snow events that cause surface soil cracking, allowing CH_4 to escape (Song et al., 2012; Tagesson et al., 2012; Raz-Yaseef et al.,2017;Pirk et al., 2017).

The patterns of CH_4 emissions at EML strongly suggest the presence of a stored reservoir of CH_4 in the winter season. There were two pulses of CH_4 released in May of 2016 during spring thaw, which we hypothesize was the release of stored CH_4 produced during the previous shoulder season (Figure 3). There was no similar spring CH_4 thaw release during the 2017 season (Figure 2d). The differences in these two spring thaw emissions could be due to the series of large CH_4 pulses in December-January 2016/2017 in response to abrupt air and shallow soil temperature warming, depleting stored CH_4 prior to spring thaw (Figure 4). Collection of a longer time series should allow us to evaluate the antecedent effects of winter emissions on the strength of the following spring season thaw emissions.

Table 5
Annual Weekly Mean Predictor Variables of CH Regression Model

A) Response variable	Full model	Variable removed	AIC	R2	R2 Adjusted
Median weekly CH4 flux (mg C-CH4 m-2 30 min-1)	All variables		-186.6	0.56	0.53
		VWC	-181.7	0.5	0.48
B) Response variable	Final model	Coefficient	AIC	R2	R2 Adjusted
Median weekly CH4 flux (mg C-CH4 m-2 30 min-1)	Intercept **	0.038±(0.012)	-186.6	0.56	0.53
	DST***	0.025±(0.006)			
	SST**	- 0.010±(0.003)			
	VWC *	0.081±(0.031)			

Note. Backward stepwise model selection was used to obtain final model.
DST is deep soil temperatures (°Q, SST is shallow soil temperatures (°Q.
VWC is volumetric soil moisture (%).
Variable significance:*** 0.001, ** 0.01, and * 0.05.
Full model: CH4 = intercept + DST + SST + VWC.

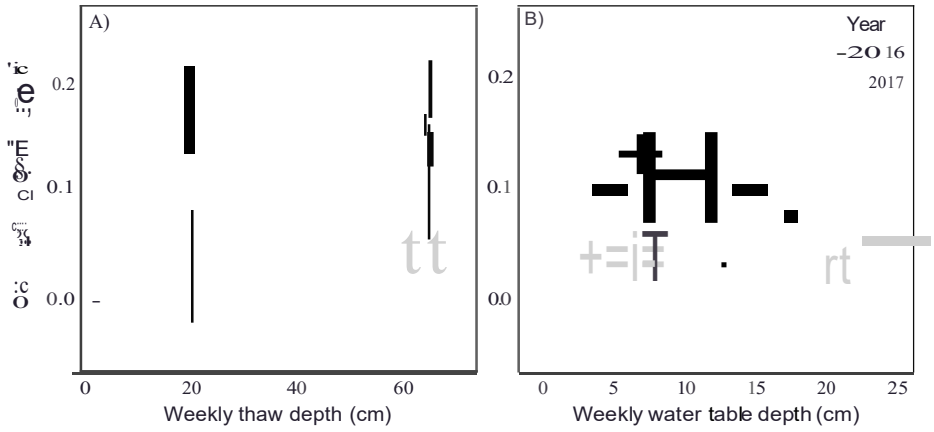

Figure 6. Weekly mean (a) thaw depths and (b) water table depth measured during the growing seasons of 2016 (filled circles) and 2017 (open circles) plotted against median weekly CH4 fluxes. Regression lines (solid line, 2016; dashed line, 2017) are the predicted model (table 6).

Methane pulses during the winter of 2016/2017 were an order of magnitude larger when the entire soil column was frozen relative to pulses in other seasons when shallow soil temperatures were above freezing. Larger winter pulses might be related to the reduced likelihood of CH_4 oxidation as it escapes frozen soil in winter. An additional explanation for the magnitude of CH_4 released in winter could be related to the lack of autumnal freeze-in bursts and low-level zero curtain emissions at EML. Autumnal bursts occur in regions underlain by permafrost, where CH_4 gas compression can occur as soilwater freezes. Freezing soils can cause ground cracking, allowing gases to escape and resulting in significant release (Mastepanov et al., 2013;Pirk et al.,2015).

At EML,deeper soils maintained temperatures within the zero curtain throughout the shoulder season,yet fluxes out of the soil remained low from October until the end of December (Figure 4a). There was also no evidence for large autumnal bursts at the end of the 2016 growing season. This suggests that the relatively large emissions in December/January were a relatively large reservoir of stored CH_4 that had accumulated in

Table 6
Growing Season Weekly Mean Predictor Variables of CH_4 Flux From Linear Mixed Effects Model

A) Response variable	Full model: maximum likelihood	Variable removed	AIC	R2 Marginal	R2 Conditional
Median weekly CH4 flux (mg C-CH4 m-2 30 min-1)	All variables		-173.3	0.55	0.59
		VWC	-175.3	0.54	0.59
		Precip	-177.0	0.55	0.59
		SST	-178.6	0.52	0.59
		DST	-180.6	0.52	0.59
		TD	-150.3	0.06	0.34
		WTD			
B) Response variable	Final model: restricted maximum likelihood	Coefficient	AIC	R2 Marginal	R2 Conditional
Median weekly CH4 flux (mg C-CH4 m-2 30 min-1)	Intercept	0.011±(0.017)	-146.5	0.46	0.61
	TD***	0.002±(0.000)			
	WTD	-0.002±(0.001)			

Note. Backward stepwise model selection was used to obtain final model.
VWC is volumetric soil moisture (%), Precip is weekly cumulative precipitation (cm), SST is shallow soil temperatures (°C), DST is deep soil temperatures (°C), TD is thaw depth (cm), and WTD is depth to water table (cm). Variable significance: *** 0.001, ** O.Dl, and * 0.05.
Full model: CH4 = intercept + VWC + Precip + SST + DST + TD + WTD; random = season.

deep soils during the zero curtain. We hypothesize that because of the late snow year and rapid freeze down of the surface soils, CH_4 produced during the shoulder season remained trapped below the frozen surface soils until it was released rapidly as air temperatures warmed rapidly. These pulses were ephemeral and only occurred during 1 week of the year, yet the magnitude (up to 105 mg $\cdot m^2 \cdot hr$) surpassed what is defined to constitute maximum biogenic fluxes in arctic permafrost systems (50 mg $\cdot m^2 \cdot$ hr; Kohnert et al., 2017). Nongrowing season burst emissions in the Arctic exhibit considerable interannual variability (Raz-Yaseef et al., 2017; Pirk et al., 2017), and longer-term observational records will help to determine whether winter pulses of this magnitude are associated with late snow years or if they are a common component of CH_4 fluxes at EML

4.4. Growing Season Methane Emissions

A synthesis of plot level CH_4 fluxes in permafrost regions identified soil temperature, soil moisture, and vegetation composition as key environmental variables that control growing season emissions (Olefeldt et al., 2012). Temperature and WTD are synergistic; the effects of temperature may become more important if WTD is at or above a certain level-acting as an "on-off" switch for emissions (Christensen et al., 2003; McEwing et al., 2015). Drier tundra systems like EML with deeper WTD (6-17 cm) may be more sensitive to changes in the position of the water table, where a 5-cm rise can increase emissions up to 45%, in contrast to inundated wetland tundra systems (WTD at 0 cm) that are more temperature sensitive (Olefeldt et al., 2012). Methane uptake was more prevalent in the drier growing season of the two growing seasons measured (27.2% in 2017 versus 10.6% in 2016; Table 3), but within each growing season weekly CH_4 fluxes did not appear to be responsive to changes in WTD position. Although WTD sometimes ranged from 10 to 20 cm for several consecutive weeks (Figure 2a), CH_4 fluxes were relatively insensitive to changes in soil moisture and WTD (Figure 6).

Net growing season CH_4 fluxes were positive and increased linearly during the growing seasons of 2016 and 2017. We hypothesized that CH_4 fluxes would be responsive to environmental drivers that typically control CH_4 fluxes and promote CH_4 production and transport. However, while soil moisture, soil temperatures, cumulative precipitation, and peak biomass were all most favorable to CH_4 emissions in mid-July, peak emissions occurred in late August through early September during both growing seasons and correlated best with weekly thaw depths above all other measured site variables (Figure 6).

Both shallow and, to a lesser extent, deep soil temperatures demonstrated some degree of hysteresis annually, where late season emissions were higher than early season emissions at the same soil temperatures (Figure 5). Hysteresis has been documented on a diurnal basis in CO_2 efflux in permafrost soils (Fouche et al., 2017) where there was a lagged disconnect between air or soil temperatures and ecosystem respiration. However, CH_4 emissions have less well understood hysteresis dynamics. Lagged emissions have been shown over the growing season with respect to water table depths (Moore & Roulet, 1993), gross primary productivity (Rinne et al., 2018), and annually with soil temperatures (Zona et al., 2016). At Ivotuk, a dry, upland tundra site similar to EML, strong seasonal hysteresis was attributed to stronger spring CH_4 oxidation, while later in the season more CH_4 is stored in the deeper active layer (Zona et al., 2016). The mechanism may be applicable at EML too, where hysteresis appears to be mediated by depth of thaw. Lower CH_4 fluxes were measured when shallow soil temperatures averaged ~5 °C and thaw depth was shallower than 25 cm. Even as shallow soil temperatures peaked at 10.9 °C during week 28, fluxes increased weekly through the growing season as thaw deepened. Maximum growing season CH_4 fluxes from late August to September occurred when shallow soil temperatures returned to lower values (~5 °C), during maximum thaw depth. Therefore, diffusive fluxes of CH_4 (as opposed to the larger pulses) appear to be responsive to changes in temperature, but this relationship is mediated by a larger volume of unfrozen soil that likely produces and stores more CH_4 later in the growing season.

Thaw depth is observed to be an important control on CH_4 fluxes in more northerly Alaskan tundra sites during the growing season (Sturtevant et al., 2012; von Fischer et al., 2010; Zona et al., 2009, 2016). Thaw depth integrates important variables for CH_4 emissions like soil temperature and moisture and increases the volume of unfrozen organic matter available for decomposition (Olefeldt et al., 2012; Zona et al., 2009). Increased soil heat conduction to deeper soil layers through wetter conditions further deepens soil thaw during the growing season (Sturtevant et al., 2012). The rate of thaw depth may also have affected

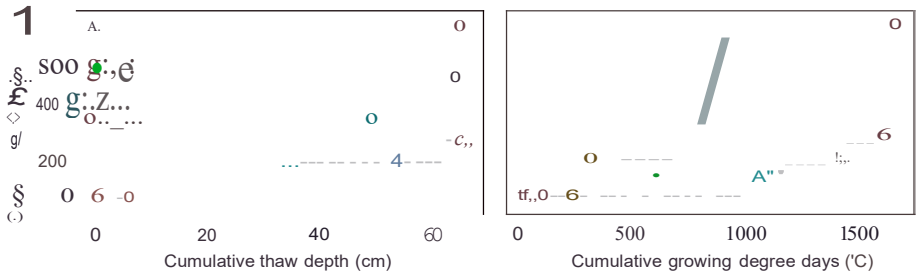

Figure 7.Monthly cumulative (a) thaw depths and (b) growing degree days plotted against cumulative monthly CH_4 fluxes during the 2016 (solid line) and 2017 (dashed line) growing seasons. Colors refer to different months measured in 2016 (circles) and 2017 (triangle).

cumulative growing season emissions, which were more than twice as high in 2016 (653.3 ± 3.9 mg C-CH_4 m^{-2}) as in 2017 (280.2 ± 3.9 mg C-CH_4 m^{-2}).While active layer thickness was not significantly different between years, the rate of thaw lagged by a month in 2017 relative to 2016 (Figure 7). This relationship is also reflected in the number of cumulative growing degree days in each growing season (Figure 7) and appeared to affect the total seasonal emissions magnitude.This is similar to findings in high Arctic tundra sites where higher cumulative CH_4 emissions tend to be related with higher total growing degree days (Pirk et al., 2017). This is not to rule out the additional effect of overall growing season moisture on cumulative CH_4 emissions. The 2017 growing season was significantly drier than 2016 (Figures 2a, 2b, and 2e and Table 2). While precipitation and soil moisture measurements were not predictive of CH_4 emissions within a growing season, there is evidence of greater CH_4 uptake in 2017,and perhaps this also affected production rates.

4.5. Net Carbon Budget

Eddy covariance data from May 2016 to April 2017 show that EMLwas a $C0_2$ net source (12.7 g C m^2/yr) with cumulative emissions about 10 times greater than CH_4 emissions (1.2 g ± 0.011 CH_4-C m^2/yr) during the same interval. Converting CH_4 to $C0_2$ equivalents and adding to the C budget results in total emissions strength of 32.3 g C m^2/yr, where CH_4 makes up 61% of annual emissions. Soils at EML were historically an active C sink since the early Holocene and until surface C accumulation stopped 8-18 years ago (Hicks Pries et al., 2012) coincident with an increase in permafrost warming (Osterkamp et al., 2009). Annual $C0_2$ balance measured and modeled at EML is strongly dependent on winter ecosystem respiration (Celis et al., 2017;Trucco et al., 2012). Winter $C0_2$ flux measurements at EML have pushed the site from a net neutral or C sink to an annual source of C in all but 2 of the last 8 years measured, offsetting the capacity of tundra biomass to be a C sink during the growing season (Celis et al., 2017). Measurement of growing season $C0_2$ fluxes at an adjacent permafrost warming experiment (CiPEHR) indicates that the future intermediate stages of thaw will lead to suppression of primary production and ecosystem respiration as a result of increased ground subsidence and soil saturation (Mauritz et al., 2017). If we assume the historical baseline of growing season CH_4 emissions at EML was neutral,or a net sink like CO:u observed CH_4 emissions may be a recent change as a result of permafrost degradation. If emissions were similar to other dry or moist tundra sites, EML may have been neutral or a CH_4sink (-022 to -0.08 g CH_4-C m^2/yr; Olefeldt et al., 2012; J0rgensen et al., 2014). Assuming annual historic range of values similar to other dry or moist tundra sites with net uptake (-022 g CH_4-C m^2/yr), net neutral (0.08 g CH_4-C m^2/yr), or half of current emissions measured (0.6 g CH_4-C m^2/yr) when measured as $C0_2$ equivalents, EML might have been a strong C sink (-3.5 to -1.3 g C m^2/yr) in the past, or CH_4 emissions may have pushed the balance to a net source assuming no net $C0_2$ emissions (9.8 g C m^2/yr). The addition of CH_4 emissions to the net carbon budget suggests that the trajectory of emissions at EML will be a stronger GHG source. Preliminary measurements at CiPEHR also suggests that CH_4 emissions increased in more deeply thawed plots, suggesting that anaerobic decomposition may become increasingly important to future ecosystem C storage inthis tundra system (Natali et al., 2015).

S. Conclusions

Our results demonstrate that this upland tundra site was a net source of CH_4 emissions, with emissions almost evenly divided between the growing season (54%) and the winter season (46%). The addition of CH_4 emissions to the C budget doubles C emissions from EML when accounting for GWP. Growing season emissions suggest that both thaw depth and rate of thaw may be predictive of growing season emissions. Sites with longer records also indicate that considerable interannual variability exists in tundra CH_4 fluxes, especially in nongrowing seasons (Mastepanov et al.,2013). Nongrowing season fluxes require further work to understand the underlying mechanisms that might enable better model predictions. A longer time series will also help determine the extent to which shoulder season emissions, and the length of the zero curtain, might be mediated by interannual differences in snow cover. Like similar studies, pulses during the nongrowing season are significant and can best be captured by year round, continuous monitoring in order to characterize seasonal patterns in emissions.

Acknowledgments
This work was based in part on support provided by the following programs: U. S. Department of Energy, Office of Biological and Environmental Research, Terrestrial Ecosystem Science (TES) Program, award DE-SC0006982 and updated with DE-SC0014085 (2015-2018); National Science Foundation CAREER program, award 0747195; National Parks Inventory and Monitoring Program; National Science Foundation Bonanza Creek LTER program, award 1026415; and National Science Foundation Office of Polar Programs, award 1203777. We would like to express our gratitude for assistance from researchers and technicians from the Schuur lab and Bonanza Creek LTER. Data presented in this manuscript are archived at the Bonanza Creek LTER Data Catalog (http://www.letr.uaf.edu/data/data-catalog).

References

Aubinet, M., Grelle, A., Ibrom, A., Rannik, Ü., Moncrieff, J., Foken, T., et al. (2000). Estimates of the annual net carbon and water exchange of forests: The EUROFLUX methodology. In A. H. Fitter & D. G. Raffaelli (Eds.), *Advances in ecological research* (Vol. 30, pp. 113-175). San Diego, CA: Elsevier.

Bekryaev, R. V., Polyakov, I. V., & Alexeev, V. A. (2010). Role of polar amplification in long-term surface air temperature variations and modern Arctic warming. *Journal of Climate*, 23(14), 3888-3906. https://doi.org/10.1175/2010JCLI3297.1

Belshe, E. F., Schuur, E. A. G., & Bolker, B. M. (2013a). Tundra ecosystems observed to be CO_2 sources due to differential amplification of the carbon cycle. *Ecology Letters*, *16*, 1307-1315. https://doi.org/10.1111/ele.12164

Belshe, E. F., Schuur, E. A. G., Bolker, B. M., & Bracho, R. (2012). Incorporating spatial heterogeneity created by permafrost thaw into a landscape carbon estimate. *Journal of Geophysical Research*, *117*, G01026. https://doi.org/10.1029/2011JG001836

Belshe, E. F. Schuur, E. A. G., & Grosse, G. (2013b). Quantification of upland thermokarst features with high resolution remote sensing. *Environmental Research Letters*, *8*(3), 035016. https://doi.org/10.1088/1748-9326/8/3/035016

Bintanja, R., & Selten, F. M. (2014). Future increases in Arctic precipitation linked to local evaporation and sea-ice retreat. *Nature*, 509(7501), 479-482. https://doi.org/10.1038/nature13259

Blanc-Betes, E., Welker, J. M., Sturchio, N. C., Chanton, J. P., & Gonzalez-Meler, M. A. (2016). Winter precipitation and snow accumulation drive the methane sink or source strength of Arctic tussock tundra. *Global Change Biology*, *22*(8), 2818-2833. https://doi.org/10.1111/gcb.13242

Burba, G. G. McDermitt, D. K., Grelle, A., Anderson, D. J., & Xu, L. (2008). Addressing the influence of instrument surface heat exchange on the measurements of C02 flux from open-path gas analyzers. *Global Change Biology*, *14*(8), 1854-1876. https://doi.org/10.1111/j.1365-2486.2008.01606.x

Callaghan, T. V., Johansson, M., Brown, R. D., Groisman, P. Y., Labba, N., Radionov, V., et al. (2011). The changing face of Arctic snow cover: A synthesis of observed and projected changes. *Ambio*, 40(S1), 17-31. https://doi.org/10.1007/s13280-011-0212-y

CAVM Team (2003). Circumpolar Arctic vegetation map. (1:7,500,000 scale), conservation of Arctic Flora and Fauna (CAFF) map no. 1. U.S. Fish and Wildlife Service, anchorage, Alaska.

Celis, G., Mauritz, M., Bracho, R., Salmon, V. G., Webb, E. E., Hutchings, J., et al. (2017). Tundra is a consistent source of CO_2 at a site with progressive permafrost thaw during 6 years of chamber and eddy covariance measurements. *Joumol of Geophysical Research: Biogeasciences*, *122*, 1471-1485. https://doi.org/10.1002/2016JG003671

Christensen, T. R., Ekberg, A., Strom, L., Mastepanov, M., Panikov, N., Oquist, M., et al. (2003). Factors controlling large scale variations in methane emissions from wetlands. *Geophysical Research Letters*, *30*(7), 1414. https://doi.org/10.1029/2002GL016848

Davidson, S. J., Sloan, V. L., Phoenix, G. K., Wagner, R. Fisher, J. P., Oechel, W. C., & Zona, D. (2016). Vegetation type dominates the spatial variability in CH. emissions across multiple Arctic tundra landscapes. *Ecosystems*, *19*(6), 1116-1132. https://doi.org/10.1007/s10021-016-9991-0

D Imperio, L., Nielsen, C. S., Westergaard-Nielsen, A. Michelsen, A., & Elberling, B. (2016). Methane oxidation in contrasting soil types: Responses to experimental warming with implication for landscape-integrated CH_4 budget. *Global Change Biology*, *23*(2), 966-976. https://doi.org/10.1111/gcb.13400

Euskirchen, E. S, Bret-Harte, M. S., Shaver, G. R., Edgar, C. W., & Romanovsky, V. E. (2016). Long-term release of carbon dioxide from Arctic tundra ecosystems in Alaska. *Ecosystems*, *20*(5), 960-974. https://doi.org/10.1007/s10021-016-0085-9

Foken, T., & Wochura, B. (1996). Tools for quality assessment of surface-based flux measurements. *Agricultural ond Forest Meteorology*, 78(1-2), 83-105. https://doi.org/10.1016/0168-1923(95)02248-1

Fouche, J., Keller, C., Allard, M., & Ambrosi, J. P. (2017). Diurnal evolution of the temperature sensitivity of CO_2 efflux in permafrost soils under control and warm conditions. *Science of the Total Environment*, *581-582*, 161-173. https://doi.org/10.1016/j.scitotenv.2016.12.089

Goulden, M. L. Munger, J. W, Fan, S. M. Daube, B. C, & Wofsy, S. C. (1996). Measurements of carbon sequestration by long-term eddy covariance: Method. s and a critical evaluation of accuracy. *Global Change Biology*, *2*(3), 169-182. https://doi.org/10.1111/j.1365-2486.1996.tb00070.x

Grosse, G, Harden, J., Turetsky, M, McGuire, A. D., Camill, P. Tarnocai, C, et al. (2011). Vulnerability of high-latitude soil organic carbon in North America to disturbance. *Journal of Geophysical Research*, *116* GOOK06. https://doi.org/10.1029/2010JG001507

Hicks Pries, C. E, Schuur, E. A. G, & (rummer, K. G. (2012). Holocene carbon stocks and carbon accumulation rates altered in soils undergoing permafrost thaw. *Ecosystems*, 75(1), 162-173. https://doi.org/10.1007/s10021-011-9500-4

Hollinger, D. Y., & Richardson, A. D. (2005). Uncertainty in eddy covariance measurements and its application to physiological models. *Tree Physiology*, *25*(7), 873-885. https://doi.org/10.1093/treephys/25.7.873

Hugelius, G., Strauss, J., Zubrzycki, S., Harden, J. W., Schuur, E. A.G., Ping, C. L. et al. (2014). Estimated stocks of circumpolar permafrost carbon with quantified uncertainty ranges and identified data gaps. *Biogeasciences*, *11*(23), 6573-6593. https://doi.org/10.5194/bg-11-6573-2014

Johansson, M., Callaghan, T. V., Bosio, J., Akerman, H. J., Jackowicz-Korczynski, M., & Christensen, T. R. (2013). Rapid responses of permafrost and vegetation to experimentally increased snow cover in sub-arctic Sweden. *Environmental Research Letters, 8(3)*, 035025. https://doi.org/10.1088/1748-9326/8/3/035025

Jorgensen, C. J., Johansen, K. M. L., Westergaard-Nielsen, A., & Elberling, B. (2014). Net regional methane sink in High Arctic soils of northeast Greenland. *Nature Geoscience*, 8(1), 20-23. https://doi.org/10.1038/ngeo2305

King, J. Y., Reeburgh, W. S., & Regli, S. K. (1998). Methane emission and transport by arctic sedges in Alaska: Results of a vegetation removal experiment. *Journal of Geophysical Research, 103(D22), 29,083-29,092*. https://doi.org/10.1029/98JD00052

Kljun, N., Calanca, P., Rotach, M. W., & Schmid, H. P. (2004). A simple parameterisation for flux footprint predictions. *Boundary-Layer Meteorology, 112(3)*, 503-523. https://doi.org/10.1023/B:BOUN.0000030653.71031.96

Kohnert, K., Serafimovich, A., Metzger, S., Hartmann, J. X. R., & Sachs, T. (2017). Strong geologic methane emissions from discontinuous terrestrial permafrost in the Mackenzie Delta, Canada. *Scientific Reports, 7*(1), *5828-5826*. https://doi.org/10.1038/s41598-017-05783-2

Kormann, R., & Meixner, F. X. (2001). An analytical footprint model for non-neutral stratification. *Boundary-Layer Meteorology*, 99(2), 207-224. https://doi.org/10.1023/A:1018991015119

Lawrence, D. M., Koven, C. D., Swenson, S. C., Riley, W. J., & Slater, A. G. (2015). Permafrost thaw and resulting soil moisture changes regulate projected high-latitude CO_2 and CH_4 emissions. *Environmental Research Letters, 10(9)*, 094011. https://doi.org/10.1088/1748-9326/10/9/094011

Lee, H., Schuur, E. A. G., Vogel, J. G., Lavoie, M., Bhadra, D., & Staudhammer, C. L. (2011). A spatially explicit analysis to extrapolate carbon fluxes in upland tundra where permafrost is thawing. *Global Change Biology, 17(3)*, 1379-1393. https://doi.org/10.1111/j.1365-2486.2010.02287.x

Mastepanov, M., Sigsgaard, C., Dlugokencky, E. J., Houweling, S., Strom, L., Tamstorf, M. P., & Christensen, T. R. (2008). Large tundra methane burst during onset of freezing. *Nature*, 456(7222), 628-630. https://doi.org/10.1038/nature07464

Mastepanov, M., Sigsgaard, C., Tagesson, T., Striim, L., Tamstorf, M. P., Lund, M., & Christensen, T. R. (2013). Revisiting factors controlling methane emissions from high-Arctic tundra. *Biogeosciences, 10(7)*, 5139-5158. https://doi.org/10.5194/bg-10-5139-2013

Mauder, M., & Foken, T. (2006). Impact of post-field data processing on eddy covariance flux estimates and energy balance closure. *Meteorologische Zeitschrift, 15(6)*, 597-609. https://doi.org/10.1127/0941-2948/2006/0167

Mauritz, M., Bracho, R., Celis, G., Hutchings, J., Natali, S. M., Pegoraro, E. P., et al. (2017). Nonlinear CO_2 flux response to 7 years of experimentally induced permafrost thaw. *Global Change Biology, 23(9)*, 3646-3666. https://doi.org/10.1111/gcb.13661

Maynes, S., Yang, F., & Parkhurst, A. (2017). hysteresis: Tools for Modeling Rate-Dependent Hysteretic Processes and Ellipses. R package version 2.6. Retrieved from https://CRAN.R-project.org/package=hysteresis

McEwing, K. R., Fisher, J. P., & Zona, D. (2015). Environmental and vegetation controls on the spatial variability of CH_4 emission from wet-sedge and tussock tundra ecosystems in the Arctic. *Plant and Soil, 38B(1-2)*, 37-52. https://doi.org/10.1007/s11104-014-2377-1

McGuire, A. D., Christensen, T. R., Hayes, D., Heroult, A., Euskirchen, E., Kimball, J. S., et al. (2012). An assessment of the carbon balance of Arctic tundra: Comparisons among observations, process models, and atmospheric inversions. *Biogeosciences*, 9(8), 3185-3204. https://doi.org/10.5194/bg-9-3185-2012

Moore, T. R., & Roulet, N. T. (1993). Methane flux: Water table relations in northern wetlands. *Geophysical Research Letters, 20(7), 587-590*. https://doi.org/10.1029/93GL00208

Myhre, G., Samset, B. H., Schulz, M., Balkanski, Y., Bauer, S., Berntsen, T. K. et al. (2013). Radiative forcing of the direct aerosol effect from AeroCom Phase II simulations. *Atmospheric Chemistry and Physics, 13(4)*, 1853-1877. https://doi.org/10.5194/acp-13-1853-201

Natali, S. M., Schuur, E. A. G., Mauritz, M., Schade, J. D., Celis, G., Crummer, K. G. et al. (2015). Permafrost thaw and soil moisture driving CO_2 and CH_4 release from upland tundra. *Journal of Geophysical Research: Biogeosciences, 120*, 525-537. https://doi.org/10.1002/(ISSN)2169-8961

Nauta, A. L., Heijmans, M. M. P. D., Blok, D., Limpens, J., Elberling, B., Gallagher, A., et al. (2015). Permafrost collapse after shrub removal shifts tundra ecosystem to a methane source. *Nature Climate Change, 5*(1), 67-70. https://doi.org/10.1038/nclimate2446

Neubauer, S. C., & Megonigal, J. P. (2015). Moving beyond global warming potentials to quantify the climatic role of ecosystems. *Ecosystems, 18(6)*, 1000-1013. https://doi.org/10.1007/s10021-015-9879-4

Olefeldt, D., Goswami, S., Grosse, G., Hayes, D., Hugelius, G., Kuhry, P. et al. (2016). Circumpolar distribution and carbon storage of thermokarst landscapes. *Nature Communications*, 7, 1-11. https://doi.org/10.1038/ncomms13043

Olefeldt, D., Turetsky, M. R., Crill, P. M., & McGuire, A. D. (2012). Environmental and physical controls on northern terrestrial methane emissions across permafrost zones. *Global Change Biology, 19(2)*, 589-603. https://doi.org/10.1111/gcb.12071

Osterkamp, T. E., Jorgenson, M. T., Schuell, E. A. G., Shur, Y. L., Kanevskiy, M. Z., Vogel, J. G., & Tumskoy, V. E. (2009). Physical and ecological changes associated with warming permafrost and thermokarst in Interior Alaska. *Permafrost and Periglacial Processes, 20(3)*, 235-256. https://doi.org/10.1002/ppp.656

Osterkamp, T. E., & Romanovsky, V. E. (1999). Evidence for warming and thawing of discontinuous permafrost in Alaska. *Permafrost and Periglacial Processes*, 70(1), 17-37. https://doi.org/10.1002/(SICI)1099-1530(199901/03)10:1<17::AID-PPP303>3.0.CO;2-4

Outcalt, S. I., Nelson, F. E., & Hinkel, K. M. (1990). The zero-curtain effect: Heat and mass transfer across an isothermal region in freezing soil. *Water Resources Research, 26(7)*, 1509-1516.

Pinheiro, J., Bates, D., DebRoy, s. Sarkar, D., & Core Team, R. (2017). Nlme: Linear and nonlinear mixed effects models. *R package version*, 3, 1-131. Retrieved from https://cran.r-project.org/package=nlme

Pirk, N., Mastepanov, M., Lopez-Blanco, E., Christensen, L. H., Christiansen, H. H., Hansen, B. U., et al. (2017). Toward a statistical description of methane emissions from arctic wetlands. *Ambio*, 46(S1), 70-80. https://doi.org/10.1007/s13280-016-0893-3

Pirk, N., Santos, T., Gustafson, J., Johansson, A. J., Tufvesson, F., Parmentier, F.-J. W., et al. (2015). Methane emission bursts from permafrost environments during autumn freeze-in: New insights from ground-penetrating radar. *Geophysical Research Letters, 42*, 6732-6738. https://doi.org/10.1002/(ISSN)1944-8007

R Core Team (2017). R: A language and environment for statistical computing. Vienna, Austria: R Foundation for Statistical Computing.

Raz-Yaseef, N., Torn, M. s. Wu, Y., Billesbach, D. P., Liljedahl, A. K., Kneafsey, T. J., et al. (2017). Large CO_2 and CH_4 emissions from polygonal tundra during spring thaw in northern Alaska. *Geophysical Research Letters, 44*, 504-513. https://doi.org/10.1002/2016GL071220

Reichstein, M., Katterer, T., Andren, O., Ciais, P., Schulze, E. D., Cramer, W., et al. (2005). Temperature sensitivity of decomposition in relation to soil organic matter pools: Critique and outlook. *Biogeasciences, 2(4)*, 317-321. https://doi.org/10.5194/bg-2-317-2005

Richardson, A. D., Hollinger, D. Y., Burba, G. G., Davis, K. J., Flanagan, L. B., Katul, G. G. et al. (2006). A multi-site analysis of random error in tower-based measurements of carbon and energy fluxes. *Agricultural and Forest Meteorology*, 736(1-2), 1-18. https://doi.org/10.1016/j.agrformet2006.01.007

Rinne, J., Tuittila, E.-s. Peltola, O., Li, X., Raivonen, M., Alekseychik, P. et al. (2018). Temporal variation of ecosystem scale methane emission from a boreal fen in relation to temperature, water table position, and carbon dioxide fluxes. *Global Biogeochemical Cycles*. https://doi.org/10.1029/2017GB005747

Romanovsky, V.E, & Osterkamp, T.E. (2000). Effects of unfrozen water on heat and mass transport processes in the active layer and permafrost. *Permafrost and Periglacial Processes*, 7 7(3), 219-239. https://doi.org/10.1002/1099-1530(200007A'.>9)113<219::AID-PPP352>3.0.C0;2-7

Schuur, E.A.G, (rummer, K G, Vogel, J.G, & Mack, M.C. (2007). Plant species composition and productivity following permafrost thaw and thermokarst in Alaskan tundra. *Ecosystems, 10(2)*, 280-292. https://doi.org/10.1007/s10021-007-9024-0

Schuur, E.A.G, McGu ire, A.D, Schadel, **C.** Grosse, G, Harden, J.W, Hayes, D.J, et al. (2015). Climate change and the permafrost carbon feedback. *Nature*, 520(7546), 171-179. https://doi.org/10.1038/naturel 4338

Schuur, E.A.G, Bockheim, J, Canadell, J.G., Euskirchen, E, Field, C. B., Goryachkin, S.V, et al. (2008). Vulnerability of permafrost carbon to climate change: Implications for the global carbon cycle. *BioScience, 58*, 701-714.

Schuur, E.A.G, Vogel, J.G., (rummer, K. G., Lee, H. Sickman, J.O, & Osterkamp, T.E. (2009). The effect of permafrost thaw on old carbon release and net carbon exchange from tundra. *Nature*, 459(7246), 556-559. https://doi.org/10.1038/nature08031

Song, C., Xu, X, Sun, X, Tian, H, Sun, L. Miao, Yet al. (2012). Large methane emission upon spring thaw from natural wetlands in the northern permafrost region. *Environmental Research Letters*, 7(3), 34009. https://doi.org/10.1088/1748-9326/7/3/034009

Sturtevant. C. **S.** Oechel, W.C, Zona, D, Kim, Y.& Emerson, C. E. (2012). Soil moisture control over autumn season methane flux, Arctic Coastal Plain of Alaska. *Biageosciences*, 9(4), 1423-1440. https://doi.org/10.5194/bg-9-1423-2012

Tagesson, T. MOider, M., Mastepanov, M, Sigsgaard, **C.** Tamstorf, M.P, Lund, M, et al. (2012). Land-atmosphere exchange of methane from soil thawing to soil freezing in a high-Arctic wet tundra ecosystem. *Global Change Biology*, 78(6), 1928-1940. https://doi.org/10.1111/j.1365-2486201202647.}(

Treat, C. C., Nata li, S.M. Ernakovich, J., Iversen, C. M, lupascu, M. McGu ire, A.D., et al. (2015). A pan-Arctic synthesis of CH_4 and $C0_2$ production from anoxic soil incubations. *Global Change Biology, 21*(7), 2787-2803. https://doi.org/10.1111/gcb.12875

Trucco, **C.** Schuur, E.A.G., Nata li, S.M., Belshe, E.F., Bracho, R. & Vogel, J. (2012). Seven-year trends of $C0_2$ exchange in a tundra ecosystem affected by long-term permafrost thaw. *Journal of Geophysical Research, 117*, G02031. https://doi.org/10.1029/2011JG001907

Vickers, D, & Mahrt, L (1997). Quality control and flux sampling problems for tower and aircraft data. *Journal of Atmospheric and Oceanic Technalagy, 14*, 512-526. https://doi.org/10.1175/1520-0426(1997)

Vogel, J, Schuur, E.A.G, Trucco, **C.** & Lee, H. (2009). Response *d* $C0_2$ exchange in a tussock tundra ecosystem to permafrost thaw and thermokarst development. *Journal of Geophysical Research, 114*, G04018. https://doi.org/10.1029/2008JG000901

Von Fischer, J.C., Rhew, R. **C.** Ames, G.M, Fosdick, B.K, & von Fischer, P.E. (2010). Vegetation height and other controls *d* spatial variability in methane emissions from the Arctic coastal tundra at Barrow, Alaska. *Journal of Geophysical Research, 115*, GOOI03. https://doi.org/10.1029/2009JG001283

Webb, E.K, Pearman, G.I, & Leuning, R. (1980). Correction of flux measurements for density effects due to heat and water vapour transfer. *Quarterly Journal of the Raya/ Meteorological Society, 106(447)*, 85-100. https://doi.org/10.1002/qj.49710644707

Whalen, S. C., & Reeburgh, W.S. (1988). A methane flux time series for tundra environments. *Global Biageochemical Cycles, 2(4)*, 399-409. https://doi.org/10.1029/GB002i004p00399

Wha len, S.**C.** Reeburgh, W.S, & Kizer, K. S. (1991). Methane consumption and emission by taiga. *Global Biogeochemical Cycks*, 5(3), 261-273. https://doi.org/10.1029/91GBO1303

Wille, C., Kutzback, L., Sachs, T, Wagner, D, & Pfeiffer, E.-M. (2008). Methane emission from Siberian arctic polygonal tundra: Eddy covariance measurements and modeling. *Global Change Biology, 14(6)*, 1395-1408. https://doi.org/10.1111/j.1365-24862008.01586J<

Wutzler, T. Reichstein, M, Mdfat, A.M, & Migliavacca, M. (2018). REddyProc :Post Processing of (Half-)Hourly Eddy-Covariance Measurements. R package version 1.1.3. Retrieved from https://cranr-project.org/package=REddyP roc

Zhang, T. (2005). Influence of the seasonal snow cover on the ground thermal regime: An overview. *Reviews of Geophysics, 43*, RG4002. https://doi.org/10.1029/2004RGOOO 157

Zhang, X, He, J, Zhang, J. Polyakov, I. Gerdes, R., Inoue, J., & Wu, P. (2013). Enhanced poleward moisture transport and amplified northern high-latitude wetting trend. *Nature Climate Change*, 3(1), 47-51 .https://doi.org/10.1038/nclimate 1631

Zona, D, Gioli, B, Com mane, R, lindaas, J, Wofsy, S.C., Miller, C. E, et al. (2016). Cold season emissions dominate the Arctic tundra methane budget. *Proceedings of the National Academy of Sciences, 113(1)*, 405. https://doi.org/10.1073/pnas.1516017113

Zona, D, Oechel, W.C, Kochendorfer, J, Paw, U. K.T. Salyuk, A N, Olivas, P.C., et al. (2009). Methane fluxes during the initiation of a large-scale water table manipulation experiment in the Alaskan Arctic tundra. *Global Biogeochemical Cycles, 23*, GB2013. https://doi.org/10.1029/2009GB003487